Supplementary Text

Constrained Motion Planning of A Cable-Driven Soft Robot With Compressible Curvature Modeling

Jiewen Lai, et al.

Dept of ME, PolyU, Hong Kong
jw.lai@connect.polyu.hk; henry.chu@polyu.edu.hk

July 2021

1 Gravitational-Elastic Energy Ratio of a Soft Segment

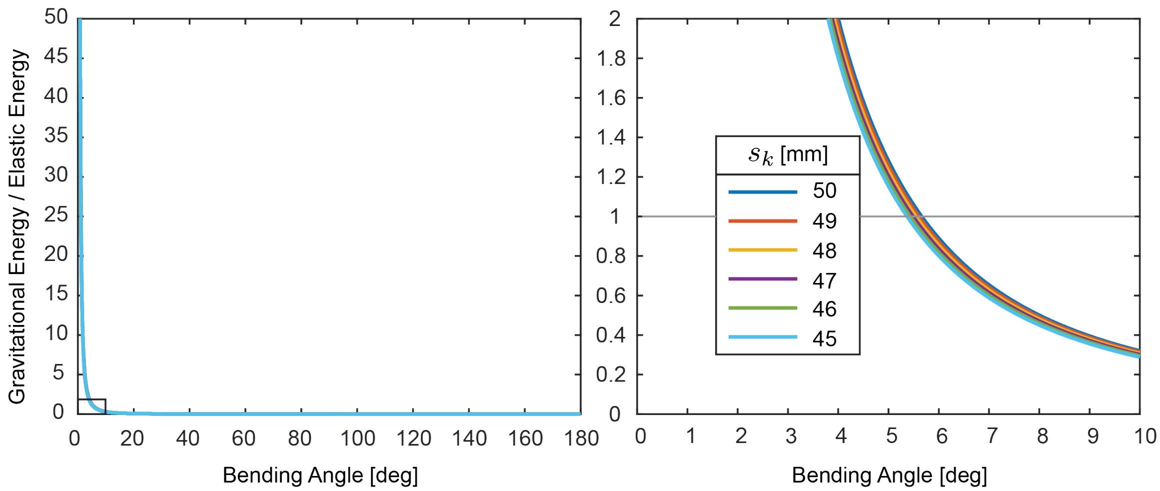

Figure 1: Gravitational-Elastic Energy Ratio of a Soft Segment

Assume that the soft segment bends as a cantilever beam, the elastic potential energy generated by the pure bending is

$$U_k = \frac{EI}{2}\int_0^{s_k}\left(\frac{\mathrm{d}\theta_k}{\mathrm{d}s}\right)^2 \mathrm{d}s = \frac{EI\theta_k^2}{2s_k} \tag{1}$$

where $E = 0.8$ MPa is the Young's modulus of the soft material, I is the cross-sectional second moments of area of an annulus with an inner radius $r_1 = 1.8$ mm and an outer radius $r_2 = 4.5$ mm as $I = \frac{\pi}{4}\left(r_2^4 - r_1^4\right)$. The net weight of a soft segment is 2.5 g. A numerical diagram of the gravitational-elastic energy ratio of a soft segment is shown in the figure above. It shows that the elastic energy starts to dominate its gravitational energy when the bending angle is greater than a small angle around 5–6 degrees.

Therefore, for our prototype, the gravity of the soft robot can be neglected.

2 Derivation of $\cos(\phi_k)$ and $\sin(\phi_k)$

From equation (6) of the main content, one can obtain

$$\cos\phi_k = \frac{f_{k,2} - 2f_{k,1} + f_{k,3}}{\sqrt{\frac{\left(3f_{k,2}-3f_{k,3}\right)^2}{3} + \left(f_{k,2} - 2f_{k,1} + f_{k,3}\right)^2}} \tag{2}$$

and

$$\sin\phi_k = \frac{\sqrt{3}\left(f_{k,2} - f_{k,3}\right)}{\sqrt{\frac{\left(3f_{k,2}-3f_{k,3}\right)^2}{3} + \left(f_{k,2} - 2f_{k,1} + f_{k,3}\right)^2}}. \tag{3}$$

3 Additional result for simulation 1

Figure 3 demonstrates the simulation results of what the orientation constraint could do to the robot motion when given a sample tip trajectory. Due to the redundancy, the robot motion will be fully bounded only when the tip orientation is specified. It shows the importance of constrained motion planning of a dexterous soft robot.

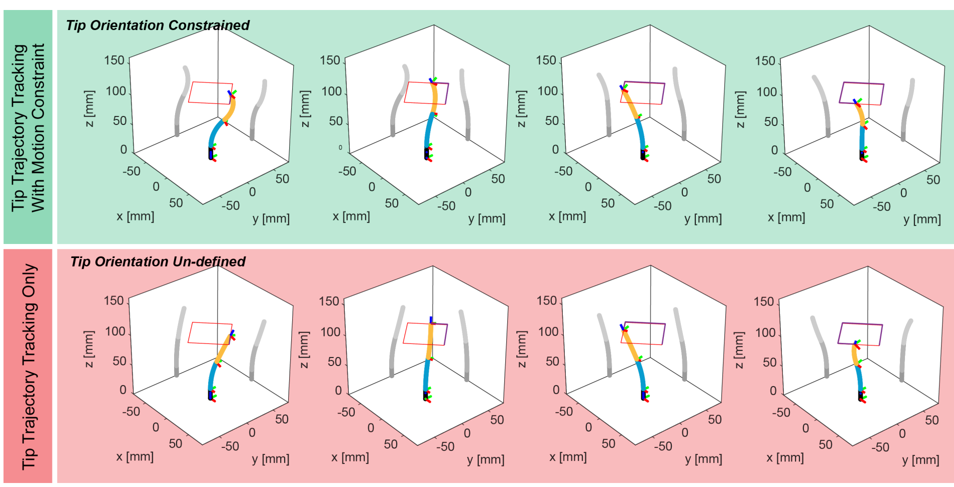

Figure 2: The soft robot tracked a square tip trajectory within its work-space. UP: The tip orientation constraint was defined as 30 degrees tilted toward [0,0,0.5236] rad (in world frame). DOWN: The tip orientation constraints was undefined. The robot motions were different despite having the same tip trajectory. The body motion matters.

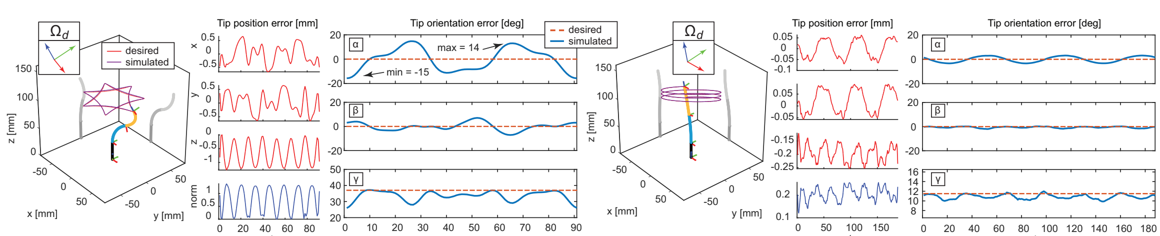

Figure 3: Simulation 1: tracking paths with the orientation of the end-effector fixed. Left: tracking a 7-corner star with the tip pointing at 37 degrees with respect to the CDSR. Right: tracking an helical oval with its tip tilted by 11.5 degrees.

4 Additional result for simulation 2

Figure 4 demonstrates the simulation results of how the collision avoidance constraint could do to the robot motion when given a sample tip trajectory.

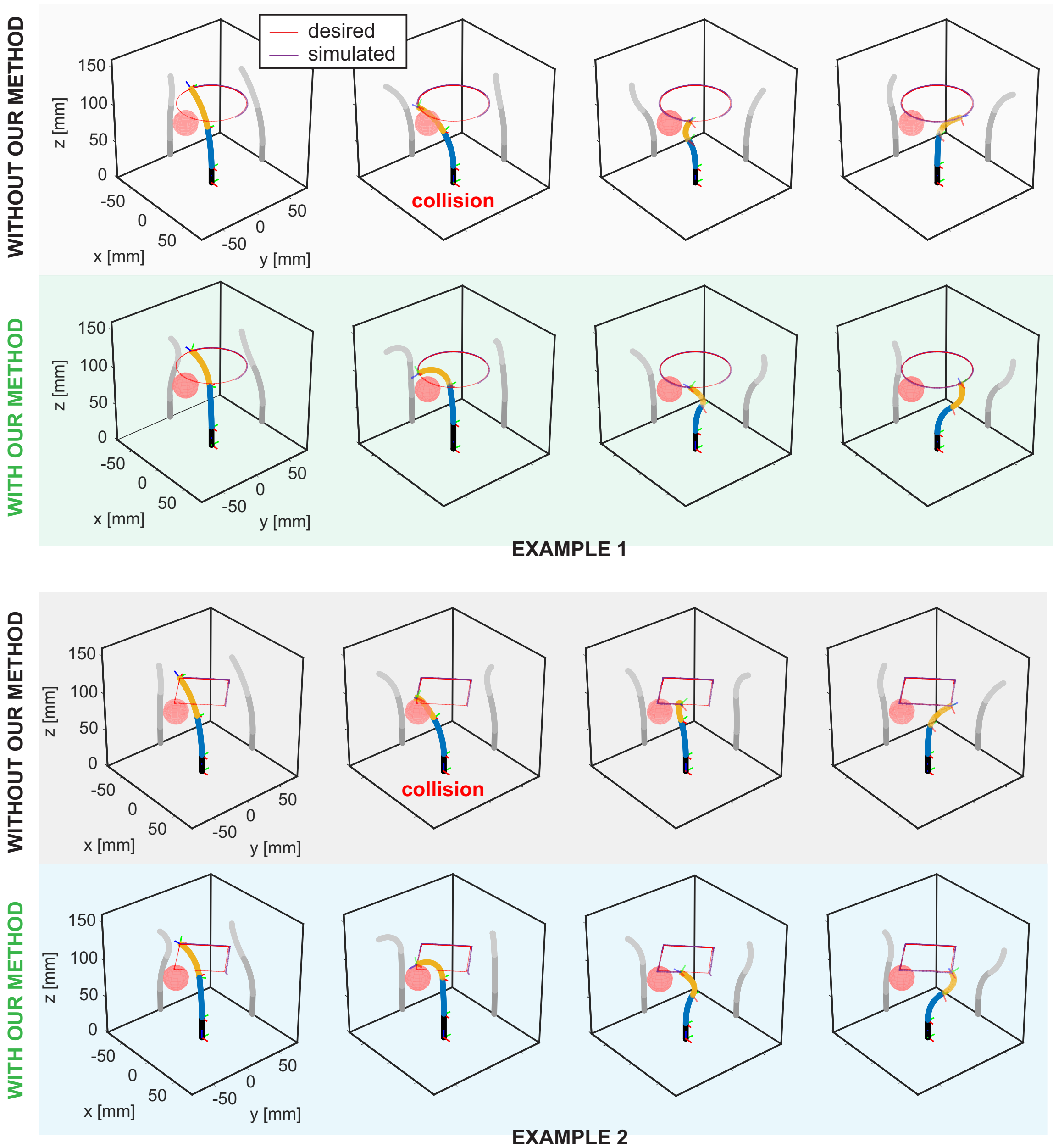

Figure 4: Simulation 2: tracking paths with the collision avoidance constraint applied. Example 1: Circular path. Example 2: Square path. The sampling steps are 45, 62, 80, and 91 out of 91 steps.

5 Derivation of the Variable Radii

Assumptions:

- *The change of the cross-sectional area is uniform throughout the local segment.*
- *The changes of the cross-sectional area at both ends are ignored.*

For a local segment of the soft body, the Poisson's ratio is defined as

$$\nu = -\frac{\varepsilon_{la}}{\varepsilon_{ax}} \tag{4}$$

where $\varepsilon_{la} > 0$ and $\varepsilon_{ax} < 0$ denotes the strain in lateral (i.e., enlarged) and axial direction (i.e., shortened) of the soft body, respectively. Under an actuation force of F, the stress of the soft body is given by

$$\sigma = \frac{F}{\mathcal{A}} \tag{5}$$

where $\mathcal{A}$ is the cross-sectional area, and thus, the axial strain is negatively defined as

$$\varepsilon_{ax} = \frac{\sigma}{E} = \frac{F}{E\mathcal{A}} < 0. \tag{6}$$

The variable length s_k can be introduced by using either the axial or lateral strain as

$$s_k = L_k + L_k \cdot \varepsilon_{ax} \tag{7}$$

or

$$s_k = L_k - L_k \cdot \frac{\varepsilon_{la}}{\nu}. \tag{8}$$

For the sake of readability, we use the subscript *prev* to represent the original dimension of a radius. Therefore, the lateral strain can be interpreted as

$$\begin{cases} \varepsilon_{la} = \dfrac{r_o - r_{o,prev}}{r_{o,prev}} \\ \\ \varepsilon_{la} = \dfrac{r_o - r_{i,prev}}{r_{i,prev}} \end{cases} \tag{9}$$

where the subscripts o and i denotes the outer and inner radius of the hollow soft body, respectively. The above equation can be associated to equations (7) and (8) and reformulated as

$$L_k - L_k \cdot \frac{r - r_{prev}}{\nu \cdot r_{prev}} = L_k + L_k \cdot \frac{F}{E\mathcal{A}}, \tag{10}$$

which can be further simplified as

$$r = r_{prev} \cdot \left(1 - \frac{F\nu}{E\mathcal{A}}\right). \tag{11}$$

Equation (11) can be explicitly interpreted at the presence of outer and inner radius as

$$\begin{cases} r_o = r_{o,prev} \cdot \left(1 - \dfrac{F\nu}{E\pi\left(r_o^2 - r_i^2\right)}\right) \\ \\ r_i = r_{i,prev} \cdot \left(1 - \dfrac{F\nu}{E\pi\left(r_o^2 - r_i^2\right)}\right) \end{cases} \tag{12}$$

Equation (12) can be solved by the symbolic solver in Matlab. Please refer to the code page.